This is an open access article published under an ACS AuthorChoice License, which permits copying and redistribution of the article or any adaptations for non-commercial purposes.

ACS OMEGA

http://pubs.acs.org/journal/acsodf

Article

Effect of Short PEG on Near-Infrared BODIPY-Based Activatable Optical Probes

Fuyuki F. Inagaki,[§] Daiki Fujimura,[§] Sara Ansteatt, Ryuhei Okada, Aki Furusawa, Peter L. Choyke, Marcin Ptaszek,* and Hisataka Kobayashi*

Cite This: *ACS Omega* 2020, 5, 15657−15665

Read Online

ACCESS | Metrics & More | Article Recommendations | Supporting Information

ABSTRACT: Targeted near-infrared (NIR) fluorescence probes are playing a significant role in biomedical imaging because NIR penetrates deeper into tissues and is associated with reduced autofluorescence compared to visible light fluorescence probes. Long-wavelength emitting 4,4-difluoro-4-bora-3a,4a-diaza-*s*-indacene (BODIPY) is an attractive platform for synthesizing NIR fluorophores because of its high photostability, high molar absorption coefficient, and sharp absorption and emission spectra. However, its lipophilicity hampers the conjugation chemistry necessary to add targeting moieties. In this study, we synthesized a novel NIR BODIPY derivative, **NMP14**. Substitutions of ethylene-bridged pyrrole units at the 3- or 5-position of the parent BODIPY chromophore result in a red shift of more than 200 nm. However, **NMP14** cannot be conjugated to antibodies because of its hydrophobicity. Therefore, we synthesized **NMP13** by adding short poly(ethylene glycol) to **NMP14** and successfully conjugated **NMP13** to cetuximab and trastuzumab. *In vitro* microscopic studies showed that **NMP13** conjugated antibodies were activated after internalization and lysosomal processing, which means that **NMP13** acts as an activatable probe only turning on after cellular internalization. After the administration of **NMP13** conjugated antibodies, mice tumors were detected with high tumor to background ratios for a long period. These results suggest that **NMP13** has potential as an activatable fluorescence probe for further clinical applications.

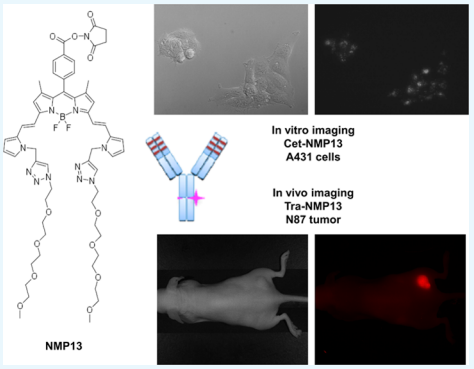

INTRODUCTION

Fluorescence imaging is a powerful tool in various fields of biomedical science. In particular, the near-infrared (NIR) wavelength I region (between 650 and 900 nm) is called the "biological window" because light in this range penetrates more deeply into tissues than visible light because of minimal absorption by water, oxy-hemoglobin, and deoxy-hemoglobin.[1] In addition, there are relatively fewer NIR auto-fluorophores in tissues, leading to reduced autofluorescence. Hence, there is increased interest in NIR fluorophores for clinical applications. The ability to target such fluorophores to specific pathologic tissues increases their potential importance.

4,4-Difluoro-4-bora-3a,4a-diaza-*s*-indacene (BODIPY) is one of the most commonly employed dyes because of its relatively high photostability, high molar absorption coefficient, and sharp absorption and emission spectra.[2] However, typical functional dyes which rely on the parent BODIPY chromophore show emission maxima in the wavelength region from 500 to 550 nm. Therefore, modifications to the BODIPY structure have been developed to create more red-shifted emitting derivatives of BODIPY. So far, aryl substitution at the 3- and/or 5-positions of the indacene skeleton,[3] styryl substitution,[4] arylethynyl substitution,[5] pyrrole substitution,[6,7] and aromatic ring fusion[8] have been reported to shift absorption and emission maxima to longer wavelengths. However, such BODIPY derivatives are highly hydrophobic, which makes conjugation with targeting moieties, including peptides and antibodies, very difficult. To improve their water solubility, the introduction of charged or water-soluble groups to BODIPY compounds has been attempted.[9,10]

In this article, we report the synthesis of *N*-hydroxysuccinimide (NHS) esters of an ethylene-bridged pyrrole-substituted BODIPY derivative (**NMP14**) and its corresponding PEGylated compound (**NMP13**), which emit NIR light. We evaluate their chemical and photophysical properties and show the feasibility of **NMP13**−antibody conjugates as activatable molecular imaging probes.

RESULTS

Molecular Design and Synthesis of Fluorophores. Installation of styryl substituents at the pyrrolic positions is a

Received: April 22, 2020
Accepted: June 5, 2020
Published: June 16, 2020

© 2020 American Chemical Society

common strategy for obtaining long-wavelength absorbing and emitting BODIPY derivatives.[11,12] Preparation of deep-red or NIR derivatives (with $\lambda_{abs/em}$ > 675 nm) requires an attachment of strongly electron-donating groups at the styryl moiety, among which the dimethylamino group offers the longest wavelength of absorption/emission (>700 nm).[13] However, [4-(*N*,*N*-dimethylaminophenyl)]vinyl-substituted BODIPYs feature a complex dependence of the emission wavelength and quantum yield on solvent pH and polarity.[13] Therefore, we have been searching for analogous, electron-rich styryl-type substituents, which afford BODIPY derivatives with NIR of absorption and emission, and high fluorescence quantum yield, regardless of the environment. Moreover, we sought for derivatives which can be straightforwardly modified by hydrophobic or hydrophilic substituents, without altering absorption and emission properties. We found, that *N*-alkyl-2-pyrrolylvinyl-substituted BODIPY derivatives absorb and emit at ∼700 nm and exhibit a relatively high fluorescence quantum yield in nonpolar and polar solvents.[14] Moreover, *N*-pyrrole substitution offers a convenient way to install a variety of groups. Accordingly, here, we examine two derivatives, **NMP13**, possessing a short poly(ethylene glycol) (PEG) chain as a *N*-pyrrole substituent, and **NMP14**, equipped with a lipophilic *N*-propargyl substituent. A PEG chain in **NMP13** is installed through click chemistry, and the resulting triazole moiety additionally increases hydrophilicity of the *N*-pyrrole substituent.

NHS esters, **NMP13** and **NMP14**, were synthesized from corresponding methyl esters, **NMP13-OMe**[14] and **NMP14-OMe**,[14] through LiOH hydrolysis of ester function and subsequent EDC-mediated coupling with NHS (Scheme 1). Absorption and emission data for **NMP13-OMe** and **NMP14-OMe** are presented in Table 1. Structures and spectral profiles of **NMP13** and **NMP14** are shown in Figure 1.

Scheme 1. Synthesis of NHS Esters NMP13 and NMP14

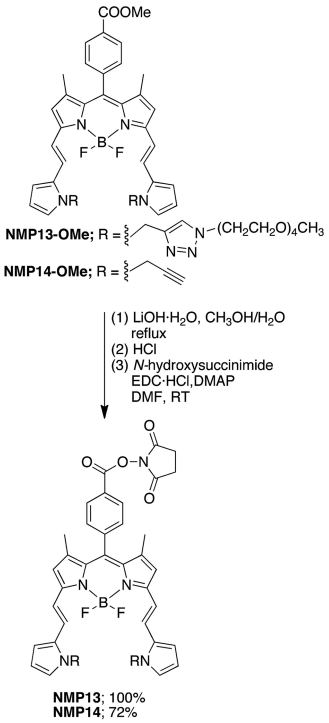

Table 1. Absorption and Emission Data for NMP13-OMe and NMP14-OMe[a,b]

compound	λ_{abs} (nm)	λ_{em} (nm)	Φ_{em}[c]
NMP13-OMe	697	721	0.40 [0.30]
NMP14-OMe	695	713	0.43 [0.34]

[a]All data are taken from ref 14. [b]All data determined in toluene. [c]Data in brackets determined in DMF.

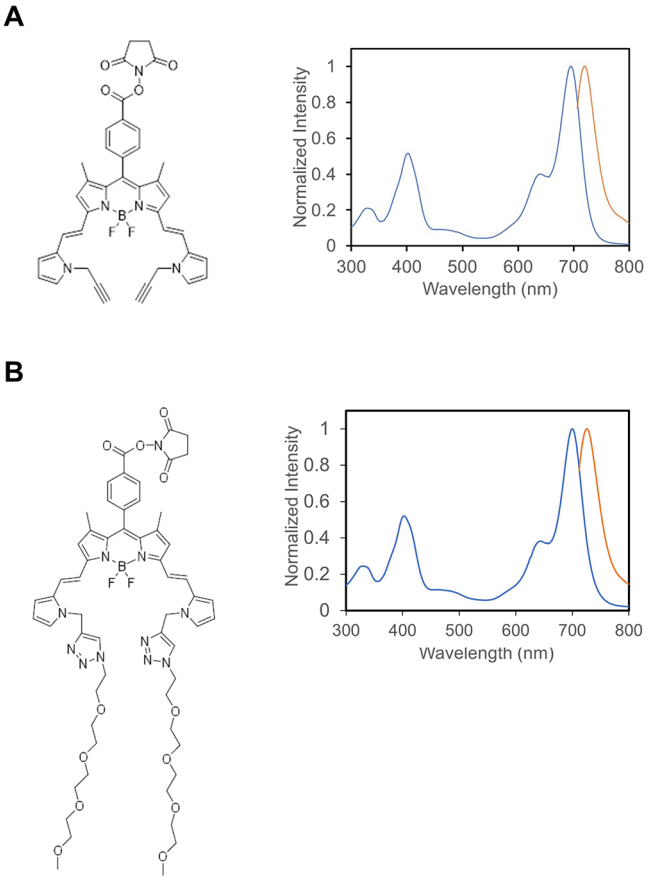

Figure 1. Chemical structures and spectral profiles of BODIPY-based derivatives, **NMP14** (A) and **NMP13** (B). Spectral profiles were measured in toluene. Light at 697 nm wavelength is used for the measurement of **NMP13** emission spectrum. Light at 695 nm wavelength is used for the measurement of **NMP14** emission spectrum.

Lipophilicity of NMP13 and NMP14. The partition coefficients of **NMP13** and **NMP14** were examined to evaluate their lipophilicity. The log *P* values (higher values indicate higher lipophilicity) were 1.80 ± 0.05 and 3.14 ± 0.18 for **NMP13** and **NMP14**, respectively, which meant that short PEG linkers successfully reduced the lipophilicity of the BODIPY-based dye.

Characteristics of NMP13 or NMP14 Conjugated Antibodies. To evaluate the characteristics of **NMP13** or **NMP14** conjugated antibodies, sodium dodecyl sulfate polyacrylamide gel electrophoresis (SDS-PAGE) and size-exclusion chromatography (SEC) were performed. The position of the **NMP13** fluorescence signal coincided with the position of the antibody band on SDS-PAGE (Figure 2A,C). The result of SEC also showed that the absorption peak at 700 nm, the maximum absorption wavelength for **NMP13**, was detected at the same position as the monomer peak eluting

https://dx.doi.org/10.1021/acsomega.0c01869
ACS Omega 2020, 5, 15657−15665

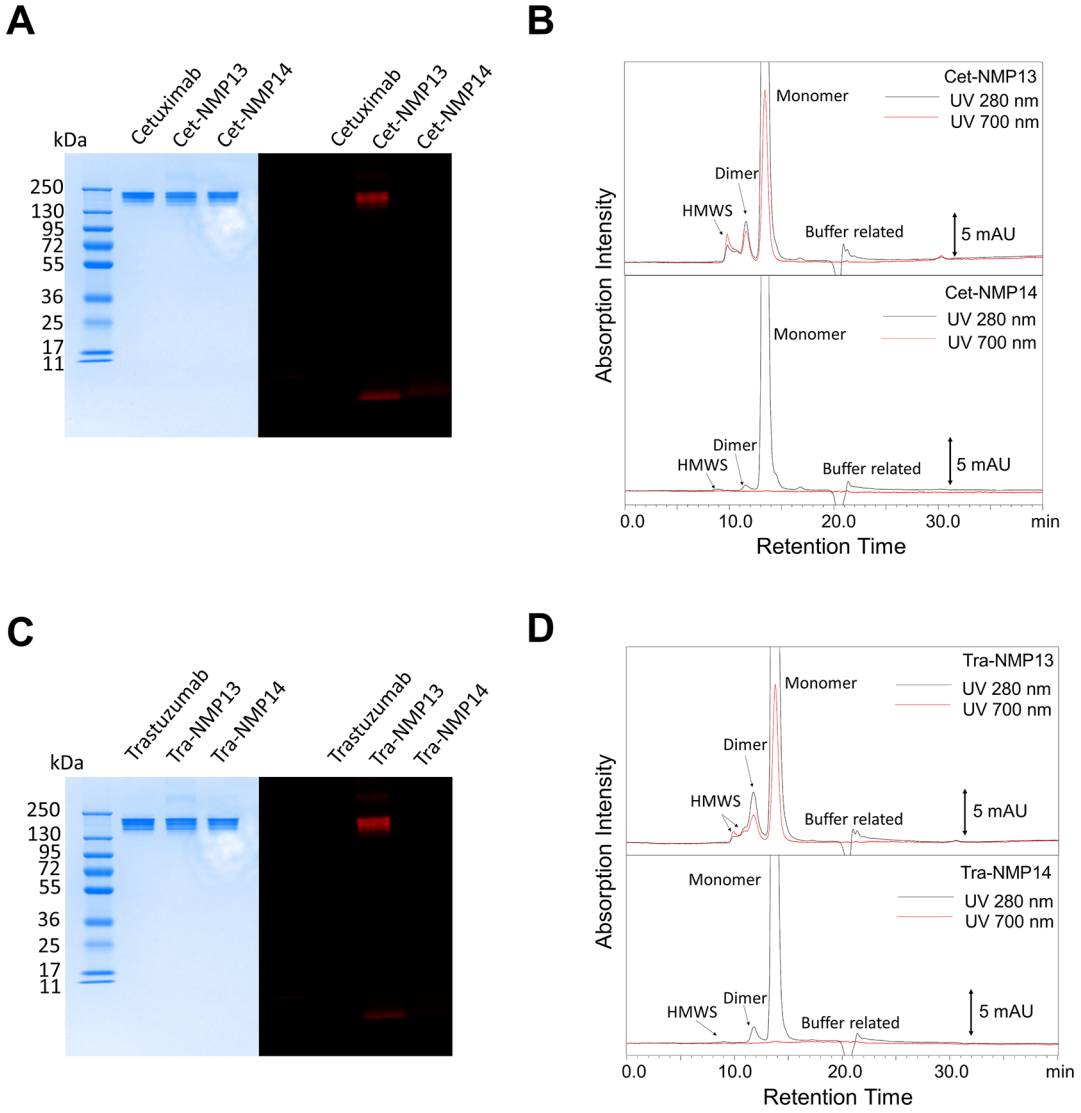

Figure 2. (A) Validation of covalently bound **NMP13** or **NMP14** to cetuximab by SDS-PAGE (left: colloidal blue staining, right: fluorescence). (B) SEC analysis of Cet-**NMP13** and Cet-**NMP14**. The absorption of the elution was monitored at wavelengths of 280 and 700 nm. (C) Validation of covalently bound **NMP13** or **NMP14** to trastuzumab by SDS-PAGE (left: colloidal blue staining, right: fluorescence). (D) SEC analysis of Tra-**NMP13** and Tra-**NMP14**. The absorption of the elution was monitored at wavelengths of 280 and 700 nm. HMWS: high molecular weight species.

at 13.7 min for both antibodies (Figure 2B,D). These results indicated that **NMP13** was reliably bound to the antibodies. On the other hand, **NMP14** revealed no fluorescence band on SDS-PAGE or no absorption peak on SEC. These results indicated that **NMP14** was not bound to antibodies. It was further observed that many water-insoluble aggregates remained on the gel-filtration column (Figure S1).

The number of **NMP13** conjugated to each antibody was quantified with the 700 nm absorption in the UV−vis system and the fluorescence intensity ratio of each band in SDS-PAGE. As defined by SDS-PAGE, the fractions of covalently bound NMP13 to cetuximab and trastuzumab were 55.5 ± 2.62 and 80.9 ± 4.18%, respectively. The number of covalently bound **NMP13** to antibody was 1.10 ± 0.10 and 1.31 ± 0.031 for Cet-**NMP13** and Tra-**NMP13**, respectively.

Dequenching Capacities of Antibody−Dye Conjugates. By adding 1% SDS to antibody−dye conjugates, dequenching capacities were observed (Figure 3A,B). The dequenching capacities were 5.73- and 6.34-fold for Cet-**NMP13** and Tra-**NMP13**, respectively. Cet-**NMP13** and Tra-**NMP13** showed 50.1 and 30.9% fluorescence recovery 4 h after incubation in mouse serum (Figure 3A−C).

***In Vitro* Observation of NMP13 Conjugates.** To evaluate the binding specificity and fluorescence intensity of antibody−**NMP13** conjugates, flow cytometric analysis was performed using A431GFP-luc, MDA-MB-468GFP-luc, and N87GFP-luc cells. A431GFP-luc and MDA-MB-468GFP-luc cells are known to express human epidermal growth factor receptor (EGFR). N87GFP-luc cells express human EGFR type 2 (HER2). The addition of excess nonconjugated antibody blocked the binding of antibody−**NMP13** conjugates (Figure 4A). Microscopy studies showed that the initial fluorescence of **NMP13** conjugated antibodies was still low after 3 h incubation but increased over time. These results suggest that each conjugate is activated after internalization and lysosomal processing (Figure 4B).

***In Vivo* Fluorescence Imaging Study.** To demonstrate *in vivo* pharmacokinetic profiles of Tra-**NMP13**, an *in vivo* imaging study was performed. Tra-**NMP13** was administered to N87GFP-luc tumor-bearing mice, and serial fluorescence

https://dx.doi.org/10.1021/acsomega.0c01869
ACS Omega 2020, 5, 15657−15665

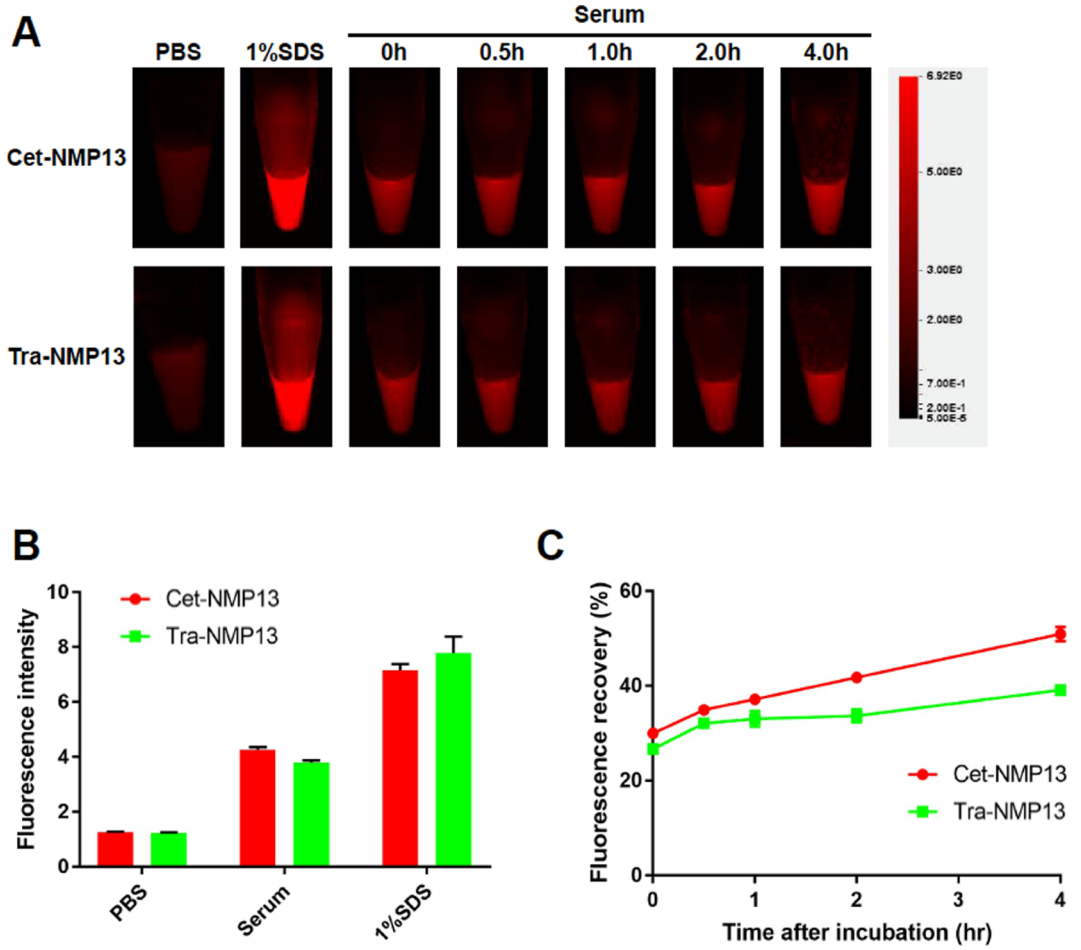

Figure 3. (A) Serial fluorescence images of dequenching properties in 1% SDS in PBS and mouse serum. (B) Comparison of fluorescence intensity of **NMP13** conjugated antibody in PBS, mouse serum, and 1% SDS in PBS. Data are presented as mean ± SEM (n = 3). (C) Fluorescence recovery in mouse serum. Data are presented as mean ± SEM (n = 3).

images were obtained (n = 7 mice per group) (Figure 5A). N87 tumors showed minimal fluorescence 3 h after administration of Tra-**NMP13**. The fluorescence intensity gradually increased and reached its peak 72 h after administration. On the other hand, the fluorescence intensity in the liver reached its peak 3 h after administration and gradually decreased (Figure 5B). The initial increase in liver fluorescence intensity was likely due to noncovalently conjugated dyes and aggregated dyes. The maximum of tumor to background ratio was 8.79 on the fifth day, and the maximum of liver to background ratio was 1.81 (Figure 5C). A high fluorescence signal was observed in small intestine and gallbladder, which indicated that **NMP13** was excreted *via* the biliary tree (Figure 5A,D).

DISCUSSION

Substitution of pyrrole at the 3- or 5-position of the parent BODIPY chromophore is an efficient method to extend the π-conjugation of the chromophore, resulting in a red shift of absorption and emission maxima. Substitution of one pyrrole produces a red shift of around 85−95 nm, and installation of pyrrole units at both positions brings a larger red shift of ∼180 nm.[11] In this study, we have synthesized novel BODIPY-based dyes by installation of ethylene-bridged pyrrole units at the 3- and 5-positions of the indacene skeleton of BODIPY. These dyes could shift their absorption and emission maxima by more than 200 nm to NIR wavelengths in nonpolar solvents.

Antibodies bind target molecules with high specificity and high sensitivity; therefore, antibody-based imaging techniques and drug delivery systems have been well studied.[15−17] The *in vitro* potency of antibody−dye or antibody−drug conjugates relies on the conjugation efficiency of dyes or drugs to the antibody. Hydrophobic ligands avoid exposure to the aqueous phase by aggregation, resulting in reduced conjugation efficiency and increasing noncovalent association to proteins. Contaminating aggregates among antibody−dye conjugates can result in a high background signal in imaging because serum albumin acts not only as a conventional binding scaffold but also as a solubilizer of dye aggregates.[18] Accordingly, hydrophilicity is one of the most important factors in successful conjugation chemistry, and various molecular modifications have been attempted to increase hydrophilicity. To this end, the addition of sulfonic acid, carbohydrate, carboxylic acid, or ammonium salt motifs to BODIPY-based dyes has been reported.[19−21] PEGylation is also a well-established method to improve *in vivo* pharmacokinetics and *in vivo* stability by conferring higher water solubility.[22−24] In this study, **NMP14** was highly hydrophobic and hardly reacted with antibodies in the aqueous phase. The addition of short PEG chains to **NMP14** increased hydrophilicity and allowed **NMP13** to conjugate to antibodies.

https://dx.doi.org/10.1021/acsomega.0c01869
ACS Omega 2020, 5, 15657−15665

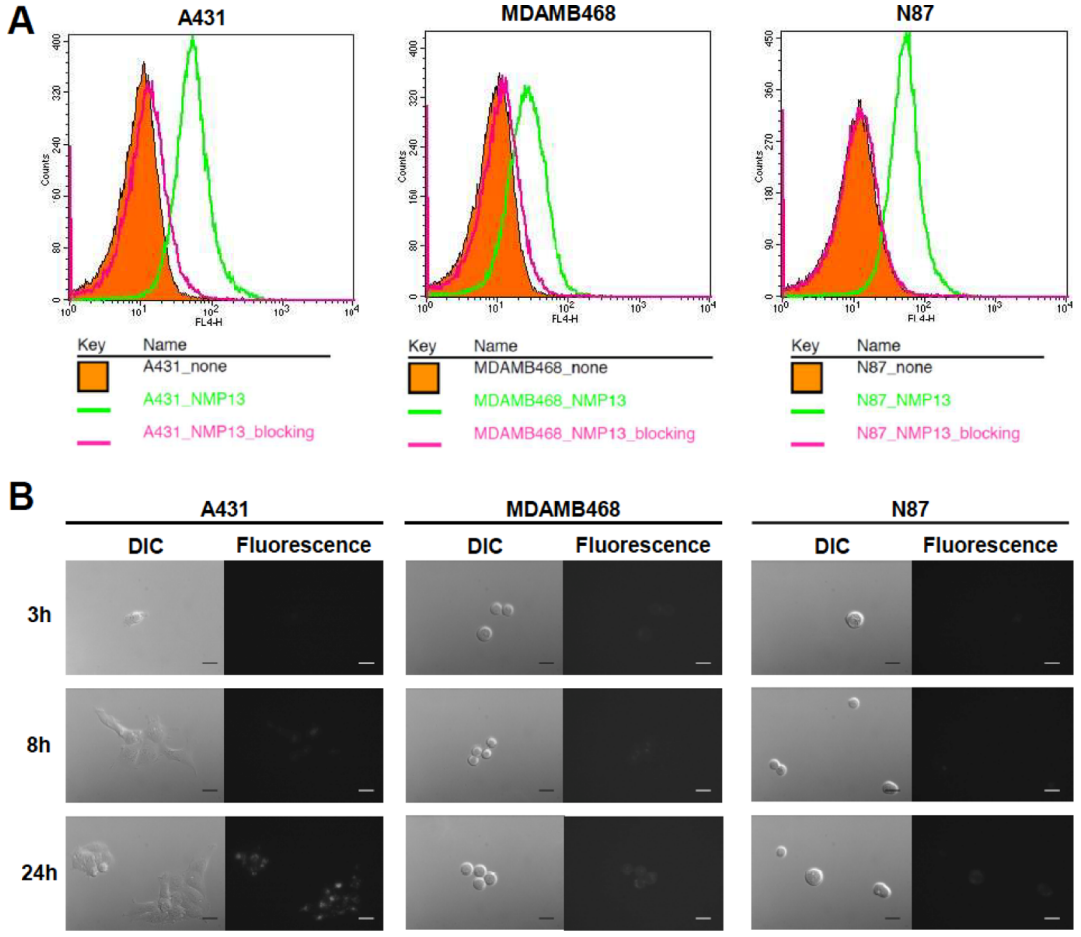

Figure 4. (A) Flow cytometric analysis of **NMP13** conjugated antibodies. A431GFP-luc cells and MDA-MB-468GFP-luc cells were incubated with Cet-**NMP13** for 2 h. N87GFP-luc cells were incubated with Tra-**NMP13** for 2 h. Preincubation with excess nonconjugated antibodies blocked the binding of **NMP13** conjugated antibody. (B) Fluorescence microscopy. A431GFP-luc cells and MDA-MB-468GFP-luc cells were incubated with Cet-**NMP13** for 3 or 8 or 24 h. N87GFP-luc cells were incubated with Tra-**NMP13** for 3 or 8 or 24 h. The fluorescent signal on the cell surface was hardly detected. The fluorescent signal was detected after internalization into the cells after 24 h incubation. Scale bar indicates 20 μm. DIC: differential interference contrast.

As shown in the microscopic studies, the fluorescence intensity of **NMP13** increased after internalization and lysosomal processing, which means that **NMP13** is activated by lysosomal processing which includes protein catabolism. Additionally, when **NMP13** is conjugated to monoclonal antibodies, the quenching mechanism of the fluorescent signal relies on the Foster resonance energy transfer (FRET) because the absorbance spectra after conjugation only showed a minimal shift to the long wavelength.[25] Dequenching of antibody−**NMP13** conjugates depends on catabolism of antibody molecules in the lysosome that physically separates **NMP13** fluorophores for suppressing FRET. Therefore, it took three days for fluorescence intensity to reach its peak *in vivo*. Additionally, **NMP13** maintained high levels of fluorescence intensity for several days probably due to its lipophilicity. Conversely, highly water-soluble always-on probes such as IRDye700DX were reported to reach their peak earlier and be cleared promptly.[26,27] Considering clinical diagnostic use, sustained accumulation of fluorescence probes in targets can be of advantage in which a strict administration schedule is not required.

In conclusion, we synthesized ethylene-bridged pyrrole-substituted BODIPY derivatives, **NMP14** and **NMP13**. Although **NMP14** could not be conjugated to antibodies because of its high hydrophobicity, we successfully conjugated **NMP13** to cetuximab and trastuzumab by the addition of short PEG linkers. **NMP13** antibody conjugates achieved a high tumor to background ratio and persistent fluorescent signal within tumors following activation.

MATERIALS AND METHODS

Reagents. Cetuximab, a chimeric (mouse/human) IgG1 mAb directed against human EGFR, was purchased from Bristol-Meyers Squibb Co. (Princeton, NJ, USA). Trastuzumab, 95% humanized IgG1 mAb against human EGFR type 2 HER2, was purchased from Genentech (South San Francisco, CA, USA). All other chemicals were of reagent grade.

Synthesis and Characterization of BODIPY Derivatives (NMP13 and NMP14). NHS esters, **NMP13** and **NMP14**, were prepared from corresponding methyl esters **NMP13-OMe** and **NMP14-OMe** for which syntheses will be reported elsewhere.[14]

NMP13. A mixture of **NMP13-OMe** (501.8 mg, 0.465 mmol) and CH_3OH/H_2O (4:1, 9 mL) was stirred and heated to reflux. In a separate flask, a mixture of $LiOH{\cdot}H_2O$ (1.35 g, 32.3 mmol) and CH_3OH/H_2O (4:1, 12 mL) was stirred at room temperature until the base dissolved completely. The $LiOH{\cdot}H_2O$ solution was transferred to the solution of

https://dx.doi.org/10.1021/acsomega.0c01869
ACS Omega 2020, 5, 15657−15665

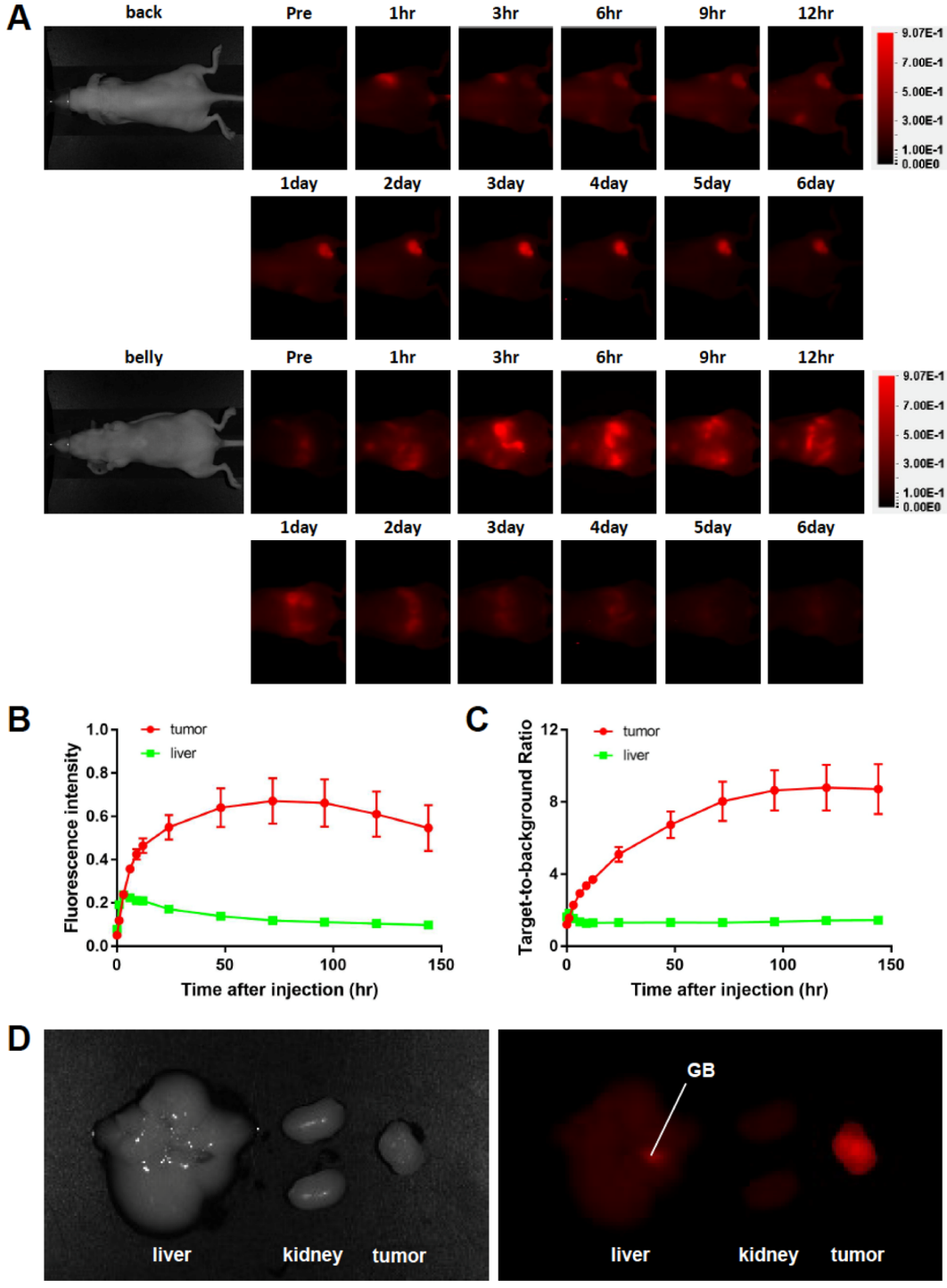

Figure 5. (A) *In vivo* serial fluorescence images of the N87GFP-luc tumor-bearing mouse, injected with Tra-**NMP13**. (B) Time course of fluorescence intensity in tumors and livers. Data are presented as mean ± SEM (n = 7 animals per time point per group). (C) Time course of TBR in tumors and livers. Data are presented as mean ± SEM (n = 7 animals per time point per group). (D) *Ex vivo* fluorescence images of the liver, kidneys, and N87GFP-luc tumor obtained 96 h after injection. GB: gallbladder.

NMP13-OMe and continued to heat at reflux for 2 h, protected from light. After reaction completion, the mixture was filtered and concentrated. The resulting product was diluted with 15 mL of water and acidified to pH ≤ 2 using 2 M HCl. The resulting solid was filtered out. The solid was collected with CH_2Cl_2, dried (Na_2SO_4), and concentrated to afford a dark green film (482.1 mg). The resulting crude acid is used in the next step without further purification. ^{1}H NMR (400 MHz, $(CD_3)_2CO$): δ 1.45 (s, 6H), 3.24 (s, 6H), 3.47 (m, 33H), 3.84 (m, 4H), 4.52 (m, 4H), 5.43 (s, 4H), 6.21 (s, 2H), 6.75 (d, J = 1.6 Hz, 2H), 6.87 (m, 2H), 7.06 (d, J = 1.9 Hz, 2H), 7.41 (d, J = 16.1 Hz, 2H), 7.65 (m, 4H), 7.88 (d, J = 2.9 Hz, 2H), 8.25 (d, J = 5.5 Hz, 2H). A mixture of a crude acid (30.1 mg, 0.028 mmol), NHS (32.5 mg, 0.283 mmol), EDC·HCl (21.7 mg, 0.113 mmol), and DMAP (13.8 mg, 0.113 mmol) in DMF (2 mL) was stirred at room temperature for 24

https://dx.doi.org/10.1021/acsomega.0c01869
ACS Omega 2020, 5, 15657−15665

h, protected from light. After reaction completion, the solution was extracted with CH_2Cl_2, washed with water (10×) and brine (1×), dried (Na_2SO_4), and concentrated to afford a dark green film (38.6 mg, ∼100% yield.) ^{1}H NMR (400 MHz, $CDCl_3$): δ 1.39 (s, 6H), 2.94 (s, 4H), 3.32 (s, 6H), 3.54 (m, 30H), 3.80 (m, 4H), 4.46 (t, J = 5.1 Hz, 4H), 5.33 (s, 4H), 6.25 (dd, J = 2.7, 3.8 Hz, 2H), 6.55 (s, 2H), 6.83 (dd, J = 1.3, 3.8 Hz, 2H), 6.88 (dd, J = 1.6, 2.5 Hz, 2H), 7.21 (d, J = 16.0 Hz, 2H), 7.38 (d, J = 15.8 Hz, 2H), 7.49 (s, 2H), 7.52 (m, 2H), 8.25 (d, J = 8.4 Hz, 2H). ^{13}C NMR (100 MHz, $CDCl_3$): δ 15.3, 26.0, 43.4, 50.7, 59.3, 69.6, 70.8, 70.8, 70.9, 72.2, 110.6, 111.9, 116.1, 118.1, 132.6, 124.3, 125.7, 125.9, 130.1, 131.4, 131.6, 132.8, 134.1, 141.0, 145.1, 153.1, 161.7, 169.5. HRMS (ESI-TOF) m/z: calculated for $C_{58}H_{70}BF_2N_{11}O_{12}$ $[M+H]^+$, 1162.5345; found, 1162.5348.

NMP14. A solution of **NMP14-OMe** (15.0 mg, 0.0245 mmol) in tetrahydrofuran (2 mL) was heated to reflux. A solid sample of $LiOH{\cdot}H_2O$ (71.4 mg, 1.70 mmol) was added to the solution followed by H_2O (2 mL). The resulting solution was heated at reflux and monitored by thin-layer chromatography until the starting material was fully consumed (3 h). After reaction completion, the mixture was filtered and concentrated. The resulting product was diluted with 3 mL of water and acidified to pH ≤ 2 using 5% HCl. The resulting mixture was extracted with CH_2Cl_2. Combined, dried (Na_2SO_4) and concentrated to afford a dark green film (21.2 mg). The resulting crude acid is used in the next step without further purification. ^{1}H NMR (400 MHz, $CDCl_3$): δ 1.42 (s, 6H), 2.47 (t, J = 2.5 Hz, 2H), 4.78 (d, J = 2.6 Hz, 4H), 6.26 (m, 2H), 6.56 (s, 2H), 6.83 (d, J = 3.6 Hz, 2H), 6.89 (m, 2H), 7.19 (d, J = 15.2 Hz, 2H), 7.47 (m, 4H), 8.23 (d, J = 8.3 Hz, 2H). A solution of the crude acid, NHS (40.8 mg, 0.354 mmol), EDC·HCl (27.2 mg, 0.142 mmol), and DMAP (17.3 mg, 0.142 mmol) in DMF (2 mL), was then stirred at room temperature for approximately 24 h, protected from light. After reaction completion, the solution was extracted with CH_2Cl_2, washed with water (10×) and brine, dried (Na_2SO_4), and concentrated. This work-up was repeated four times to remove as much free NHS as possible. Then, the resulting solid was suspended in hexanes and filtered to afford a dark green solid (12.3 mg, 72% yield.). ^{1}H NMR (400 MHz, $CDCl_3$): δ 1.43 (s, 6H), 2.48 (t, J = 2.5 Hz, 2H), 2.95 (s, 4H), 4.78 (d, J = 2.5 Hz, 4H), 6.26 (m, 2H), 6.59 (s, 2H), 6.85 (m, 2H), 6.90 (m, 2H), 7.21 (d, J = 16.0 Hz, 2H), 7.46 (d, J = 16.0 Hz, 2H), 7.54 (d, J = 8.3 Hz, 2H), 8.27 (d, J = 8.3 Hz, 2H). ^{13}C NMR (100 MHz, $CDCl_3$): δ 15.1, 25.8, 36.9, 74.4, 77.8, 86.6, 110.3, 111.9, 116.2, 117.7, 123.7, 124.9, 125.6, 129.9, 131.2, 131.4, 132.7, 134.1, 140.8, 142.8, 153.0, 161.5, 169.4. HRMS (APCI-TOF) m/z: calcd for $C_{40}H_{32}BF_2N_5O_4$ $[M + H]^+$, 696.2595; found, 696.2587.

Evaluation of the Lipophilicity of NMP13 and NMP14. The partition coefficient (log P) was determined in order to evaluate the lipophilicity of **NMP13** and **NMP14**, as described previously.[22] More specifically, each dye (50 nmol) was mixed with 1 mL each of 1-octanol and 0.1 mol/L phosphate buffer (pH 7.4) in a test tube. Three test tubes were used for each condition. The test tubes were shaken vigorously and incubated for 20 min at room temperature. This step was repeated twice to ensure that the reaction had reached equilibrium. Then, the concentration of **NMP13** and **NMP14** was determined by measuring the absorption with the UV−Vis system (8453 Value UV−Vis system, Agilent Technologies, Santa Clara, CA). The distribution ratios were calculated as the logarithm value of the octanol-to-buffer ratio (log P).

Synthesis of Fluorophore Conjugated Antibody. Antibody (1 mg, 6.8 nmol) was incubated with **NMP13** or **NMP14** (68.0 nmol in dimethyl sulfoxide) and 0.1 mol/L Na_2HPO_4 (pH 8.5) at room temperature for 120 min. The reactants were purified with the gel-filtration column (Sephadex G 25 column, PD-10, GE Healthcare, Piscataway, NJ). Unconjugated or aggregated dyes were removed by centrifugal filters (Amicon Ultra-4, 10K, MilliporeSigma, Burlington, MA) and 0.22 μm filter units (Millex-GV, MilliporeSigma). We abbreviate **NMP13** conjugated to cetuximab as Cet-**NMP13**, **NMP13** conjugated to trastuzumab as Tra-**NMP13**, **NMP14** conjugated to cetuximab as Cet-**NMP14**, and **NMP14** conjugated to trastuzumab as Tra-**NMP14**.

Liquid Chromatography Analysis. SEC analysis was performed on a Nexera XR HPLC system (Shimadzu Co., Kyoto, Japan). Approximately 25 μg of protein was loaded onto a TSKgel SuperSW 3000 (4.6 mm × 30 cm, 5 μm) with a guard column (Tosoh Bioscience, Inc., South San Francisco, CA, USA) and eluted using an isocratic flow (37 min, 0.25 mL/min) of 200 mM sodium phosphate with 10% of acetonitrile at pH 6.8. The absorption of the elution was monitored at wavelengths of 280 and 700 nm.

Quantification of the Number of Covalently Conjugated Dyes. The number of covalently conjugated dyes with each antibody was calculated by the UV−Vis system and SDS-PAGE. The absorption at 700 nm of each conjugate was measured by the UV−Vis system. Each conjugate was separated by SDS-PAGE with a 4−20% gradient polyacrylamide gel (Life Technologies, Gaithersburg, MD). After electrophoresis at 80 V for 100 min, the gel was imaged with a Pearl Imager (LI-COR Biosciences, Lincoln, NE) using an IR700 fluorescence channel (Ex; 685 nm, Em; 720 nm). Fluorescence intensity was quantified with Pearl Cam Software (LI-COR Bioscience). The gel was stained with colloidal blue staining to confirm the antibody band.

Determination of *In Vitro* Dequenching Capacity. The dequenching abilities of each conjugate were investigated by denaturation with 1% SDS, as described previously.[28] Briefly, the conjugates were mixed with phosphate-buffered saline (PBS) and 10% SDS at a ratio of 5:4:1 (the final concentration of SDS is 1%) and incubated for 20 min at room temperature. As a control, the samples were incubated in PBS without SDS. The change in fluorescence intensity was evaluated with Pearl Imager and Pearl Cam Software.

Fluorescence Recovery in Mouse Serum. Each probe was mixed with mouse serum at a ratio of 1:1, and the mixed samples were incubated at 37 °C for 0, 0.5, 1, 2, and 4 h. The change in fluorescence intensity was evaluated with Pearl Imager and Pearl Cam Software. Fluorescence recovery was calculated by the following equation: (fluorescence intensity in mouse serum − fluorescence intensity in PBS)/(fluorescence intensity in 1% SDS/PBS − fluorescence intensity in PBS) × 100.

Cell Culture. A431GFP-luc (a human epidermoid cancer cell line), MDA-MB-468GFP-luc (a human mammary cancer cell line), and N87GFP-luc (a human gastric cancer cell line) were used in this study. These cells were cultured in RPMI 1640 medium (GIBCO, Waltham, MA) supplemented with 10% fetal bovine serum (GIBCO) and 1% penicillin/

https://dx.doi.org/10.1021/acsomega.0c01869
ACS Omega 2020, 5, 15657−15665

streptomycin (GIBCO) in a humidified incubator in an atmosphere of 95% air and 5% carbon dioxide.

Flow Cytometry. *In vitro* fluorescence on cells was measured using a flow cytometer (FACSCalibur, BD BioSciences, San Jose, CA) and analyzed with CellQuest software (BD BioSciences). A431GFP-luc or MDA-MB-468GFP-luc or N87GFP-luc cells (5×10^5) were incubated with 1 μg of each conjugate for 2 h on ice. In order to validate the specific binding of the conjugated antibody, excess nonconjugated antibodies (50 μg) were added to block the conjugated antibody.

Fluorescence Microscopic Studies. A431GFP-luc or MDA-MB-468GFP-luc or N87GFP-luc cells (1×10^4) were plated on a cover glass bottomed culture plate and incubated for 24 h. Each conjugate was then added at 10 μg/mL. After 3, 8, or 24 h incubation, the cells were washed with PBS. Fluorescence microscopic images were obtained with an Olympus IX81 microscope (Olympus Corp, Tokyo, Japan). The filter set to detect **NMP13** consisted of a 590−650 nm excitation filter and a 665−740 nm band pass emission filter. Transmitted light differential interference contrast images were also acquired.

Animal Models. All animal procedures were performed in compliance with the Guide for the Care and Use of Laboratory Animal Resources (1996), the National Research Council and approved by the local Animal Care and Use Committee. Female homozygote athymic nude mice were used (Charles River, NCI-Frederick, Frederick, MD). N87GFP-luc cells (3×10^6) were subcutaneously injected into the lower flank of mice. Mice with tumors with a longitudinal diameter of about 8 mm were used for this study.

***In Vivo* Fluorescence Imaging.** Serial ventral and dorsal fluorescence images were obtained with Pearl Imager (LI-COR Bioscience, Lincoln, NE) using an IR700 fluorescence channel, before and 1, 3, 6, 9, 12, 24, 48, 72, 96, 120, and 144 h after intravenous administration of 100 μg of Tra-**NMP13** (4 mg/kg injection). For analyzing fluorescence intensities, regions of interest (ROIs) were manually drawn on tumor and liver. The average fluorescence intensities of each ROI were measured by Pearl Cam Software (LI-COR Bioscience). The target to background ratio (TBR) was calculated by the following equation: TBR = (fluorescence intensity of target)/(fluorescence intensity of background).

Statistical Analysis. Statistical analysis was performed with GraphPad Prism version 7 software (GraphPad Software, La Jolla, CA). Data are presented as mean ± standard error of mean from a minimum of three experiments unless otherwise indicated.

■ ASSOCIATED CONTENT

Supporting Information

The Supporting Information is available free of charge at https://pubs.acs.org/doi/10.1021/acsomega.0c01869.

Gel-filtration column after purification of Tra-NMP13 or Tra-NMP14 (PDF)

■ AUTHOR INFORMATION

Corresponding Authors

Marcin Ptaszek − *Department of Chemistry and Biochemistry, University of Maryland, Baltimore County, Baltimore, Maryland 21250, United States;* orcid.org/0000-0001-6468-6900; Phone: 410-455-2264; Email: mptaszek@umbc.edu

Hisataka Kobayashi − *Molecular Imaging Program, Center for Cancer Research, National Cancer Institute, National Institutes of Health, Bethesda, Maryland 20892, United States;* orcid.org/0000-0003-1019-4112; Phone: 240-858-3069; Email: kobayash@mail.nih.gov; Fax: 301-402-3191

Authors

Fuyuki F. Inagaki − *Molecular Imaging Program, Center for Cancer Research, National Cancer Institute, National Institutes of Health, Bethesda, Maryland 20892, United States*

Daiki Fujimura − *Molecular Imaging Program, Center for Cancer Research, National Cancer Institute, National Institutes of Health, Bethesda, Maryland 20892, United States*

Sara Ansteatt − *Department of Chemistry and Biochemistry, University of Maryland, Baltimore County, Baltimore, Maryland 21250, United States*

Ryuhei Okada − *Molecular Imaging Program, Center for Cancer Research, National Cancer Institute, National Institutes of Health, Bethesda, Maryland 20892, United States*

Aki Furusawa − *Molecular Imaging Program, Center for Cancer Research, National Cancer Institute, National Institutes of Health, Bethesda, Maryland 20892, United States*

Peter L. Choyke − *Molecular Imaging Program, Center for Cancer Research, National Cancer Institute, National Institutes of Health, Bethesda, Maryland 20892, United States*

Complete contact information is available at: https://pubs.acs.org/10.1021/acsomega.0c01869

Author Contributions

[§]F.F.I. and D.F. contributed equally to this work.

Notes

The authors declare no competing financial interest.

■ ACKNOWLEDGMENTS

This research was supported by the Intramural Research Program of the National Institutes of Health, National Cancer Institute, Center for Cancer Research (ZIA BC 011512). F.F.I. was also supported with a grant from the National Center for Global Health and the Medicine Research Institute, Tokyo, Japan. Work at the UMBC was supported by the National Cancer Institute of the National Institutes of Health under award number U01CA181628 (to M.P.). The content is solely the responsibility of the authors and does not necessarily represent the official views of the National Institutes of Health.

■ REFERENCES

(1) Weissleder, R. A clearer vision for in vivo imaging. *Nat. Biotechnol.* **2001**, *19*, 316−317.

(2) Treibs, A.; Kreuzer, F.-H. Difluorboryl-Komplexe von Di- und Tripyrrylmethenen. *Liebigs Ann. Chem.* **1968**, *718*, 208−223.

(3) Yamada, K.; Toyota, T.; Takakura, K.; Ishimaru, M.; Sugawara, T. Preparation of BODIPY probes for multicolor fluorescence imaging studies of membrane dynamics. *New J. Chem.* **2001**, *25*, 667−669.

(4) Rurack, K.; Kollmannsberger, M.; Daub, J. Molecular Switching in the Near Infrared (NIR) with a Functionalized Boron-Dipyrromethene Dye. *Angew. Chem., Int. Ed.* **2001**, *40*, 385−387.

(5) Rohand, T.; Qin, W.; Boens, N.; Dehaen, W. Palladium-Catalyzed Coupling Reactions for the Functionalization of BODIPY Dyes with Fluorescence Spanning the Visible Spectrum. *J. Org. Chem.* **2006**, *2006*, 4658−4663.

(6) Zhang, M.; Hao, E.; Zhou, J.; Yu, C.; Bai, G.; Wang, F.; Jiao, L. Synthesis of pyrrolyldipyrrinato BF2 complexes by oxidative nucleophilic substitution of boron dipyrromethene with pyrrole. *Org. Biomol. Chem.* **2012**, *10*, 2139−2145.
(7) Yu, C.; Miao, W.; Wang, J.; Hao, E.; Jiao, L. PyrrolylBODIPYs: Syntheses, Properties, and Application as Environment-Sensitive Fluorescence Probes. *ACS Omega* **2017**, *2*, 3551−3561.
(8) Wada, M.; Ito, S.; Uno, H.; Murashima, T.; Ono, N.; Urano, T.; Urano, Y. Synthesis and optical properties of a new class of pyrromethene−BF2 complexes fused with rigid bicyclo rings and benzo derivatives. *Tetrahedron Lett.* **2001**, *42*, 6711−6713.
(9) Bardon, K. M.; Selfridge, S.; Adams, D. S.; Minns, R. A.; Pawle, R.; Adams, T. C.; Takiff, L. Synthesis of Water-Soluble Far-Red-Emitting Amphiphilic BODIPY Dyes. *ACS Omega* **2018**, *3*, 13195−13199.
(10) Zhu, S.; Zhang, J.; Vegesna, G.; Luo, F.-T.; Green, S. A.; Liu, H. Highly water-soluble neutral BODIPY dyes with controllable fluorescence quantum yields. *Org. Lett.* **2011**, *13*, 438−441.
(11) Kadassery, K. J.; Nimesh, A.; Raj, S.; Agarwal, N. 3-/3,5-Pyrrole-substituted BODIPY derivatives and their photophysical and electrochemical studies. *J. Chem. Sci.* **2016**, *128*, 1435−1443.
(12) Lu, H.; Mack, J.; Yang, Y.; Shen, Z. Structural modification strategies for the rational design of red/NIR region BODIPYs. *Chem. Soc. Rev.* **2014**, *43*, 4778−4823.
(13) Baruah, M.; Qin, W.; Flors, C.; Hofkens, J.; Vallée, R. A. L.; Beljonne, D.; Van der Auweraer, M.; De Borggraeve, W. M.; Boens, N. Solvent and pH Dependent Fluorescent Properties of a Dimethylaminostyryl Borondipyrromethene Dye in Solution. *J. Phys. Chem. A* **2006**, *110*, 5998−6009.
(14) Ansteatt, S.; Meares, A.; Ptaszek, M. Novel Near-IR Emitting BODIPY Derivatives and Their Energy Transfer Arrays. *J. Org. Chem.*, submitted for publication.
(15) Kobayashi, H.; Choyke, P. L.; Ogawa, M. Monoclonal antibody-based optical molecular imaging probes; considerations and caveats in chemistry, biology and pharmacology. *Curr. Opin. Chem. Biol.* **2016**, *33*, 32−38.
(16) Inagaki, F. F.; Furusawa, A.; Choyke, P. L.; Kobayashi, H. Enhanced nanodrug delivery in tumors after near-infrared photo-immunotherapy. *Nanophotonics* **2019**, *8*, 1673−1688.
(17) Chau, C. H.; Steeg, P. S.; Figg, W. D. Antibody-drug conjugates for cancer. *Lancet* **2019**, *394*, 793−804.
(18) Jameson, L. P.; Smith, N. W.; Annunziata, O.; Dzyuba, S. V. Interaction of BODIPY dyes with bovine serum albumin: a case study on the aggregation of a click-BODIPY dye. *Phys. Chem. Chem. Phys.* **2016**, *18*, 14182−14185.
(19) Li, L.; Han, J.; Nguyen, B.; Burgess, K. Syntheses and spectral properties of functionalized, water-soluble BODIPY derivatives. *J. Org. Chem.* **2008**, *73*, 1963−1970.
(20) Uriel, C.; Sola-Llano, R.; Banuelos, J.; Gomez, A. M.; Lopez, J. C. A Malonyl-Based Scaffold for Conjugatable Multivalent Carbohydrate-BODIPY Presentations. *Molecules* **2019**, *24*, 2050.
(21) Tasior, M.; Murtagh, J.; Frimannsson, D. O.; McDonnell, S. O.; O'Shea, D. F. Water-solubilised BF2-chelated tetraarylazadipyrromethenes. *Org. Biomol. Chem.* **2010**, *8*, 522−525.
(22) Sano, K.; Nakajima, T.; Miyazaki, K.; Ohuchi, Y.; Ikegami, T.; Choyke, P. L.; Kobayashi, H. Short PEG-linkers improve the performance of targeted, activatable monoclonal antibody-indocyanine green optical imaging probes. *Bioconjugate Chem.* **2013**, *24*, 811−816.
(23) Hamidi, M.; Azadi, A.; Rafiei, P. Pharmacokinetic consequences of pegylation. *Drug Delivery* **2006**, *13*, 399−409.
(24) Watanabe, R.; Sato, K.; Hanaoka, H.; Harada, T.; Nakajima, T.; Kim, I.; Paik, C. H.; Wu, A. M.; Choyke, P. L.; Kobayashi, H. Minibody-indocyanine green based activatable optical imaging probes: the role of short polyethylene glycol linkers. *ACS Med. Chem. Lett.* **2014**, *5*, 411−415.
(25) Kobayashi, H.; Choyke, P. L. Target-Cancer-Cell-Specific Activatable Fluorescence Imaging Probes: Rational Design and in Vivo Applications. *Acc. Chem. Res.* **2011**, *44*, 83−90.
(26) Nagaya, T.; Sato, K.; Harada, T.; Nakamura, Y.; Choyke, P. L.; Kobayashi, H. Near Infrared Photoimmunotherapy Targeting EGFR Positive Triple Negative Breast Cancer: Optimizing the Conjugate-Light Regimen. *PLoS One* **2015**, *10*, No. e0136829.
(27) Nagaya, T.; Nakamura, Y.; Sato, K.; Harada, T.; Choyke, P. L.; Kobayashi, H. Near infrared photoimmunotherapy of B-cell lymphoma. *Mol. Oncol.* **2016**, *10*, 1404−1414.
(28) Ogata, F.; Nagaya, T.; Maruoka, Y.; Akhigbe, J.; Meares, A.; Lucero, M. Y.; Satraitis, A.; Fujimura, D.; Okada, R.; Inagaki, F.; Choyke, P. L.; Ptaszek, M.; Kobayashi, H. Activatable Near-Infrared Fluorescence Imaging Using PEGylated Bacteriochlorin-Based Chlorin and BODIPY-Dyads as Probes for Detecting Cancer. *Bioconjugate Chem.* **2019**, *30*, 169−183.

https://dx.doi.org/10.1021/acsomega.0c01869
ACS Omega 2020, 5, 15657−15665